HHS Public Access

Author manuscript

Methods Mol Biol. Author manuscript; available in PMC 2022 August 04.

Published in final edited form as:

Methods Mol Biol. 2022 ; 2435: 169–180. doi:10.1007/978-1-0716-2014-4_12.

Metabolic Imaging Using Hyperpolarization for Assessment of Premalignancy

Shivanand Pudakalakatti[#,1], **Priyank Raj**[#,1,2], **Travis C Salzillo**[1,2], **José S Enriquez**[1,2], **Dontrey Bourgeois**[1,3], **Prasanta Dutta**[1], **Mark Titus**[4], **Shayan Shams**[5], **Priya Bhosale**[2,6], **Michael Kim**[2,7], **Florencia McAllister**[2,8], **Pratip K Bhattacharya**[9,10]

[1]Department of Cancer Systems Imaging, University of Texas MD Anderson Cancer Center, Houston, TX, USA.

[2]MD Anderson Cancer Center UT Health Graduate School of Biomedical Sciences, Houston, TX, USA.

[3]Department of Statistics, Rice University, Houston, TX, USA.

[4]Department of Genitourinary Medical Oncology, University of Texas MD Anderson Cancer Center, Houston, TX, USA.

[5]Department of Biomedical Informatics, University of Texas Health Science Center, Houston, TX, USA.

[6]Department of Abdominal Imaging, University of Texas MD Anderson Cancer Center, Houston, TX, USA.

[7]Department of Surgical Oncology, University of Texas MD Anderson Cancer Center, Houston, TX, USA.

[8]Department of Clinical Cancer Prevention, University of Texas MD Anderson Cancer Center, Houston, TX, USA.

[9]Department of Cancer Systems Imaging, University of Texas MD Anderson Cancer Center, Houston, TX, USA.

[10]MD Anderson Cancer Center UT Health Graduate School of Biomedical Sciences, Houston, TX, USA.

Abstract

There is an unmet need for noninvasive surrogate markers that can help identify premalignant lesions across different tumor types. Here we describe the methodology and technical details of protocols employed for in vivo ^{13}C pyruvate metabolic imaging experiments. The goal of the method described is to identify and understand metabolic changes, to enable detection of pancreatic premalignant lesions, as a proof of concept of the high sensitivity of this imaging modality.

[#]Contributed equally.

Conflict of interest: The authors declare no conflict of interest.

Keywords

Hyperpolarization; Metabolic imaging; MRI; ^{13}C; HP-MR; Premalignancy; Early detection; Assessment of preventive responses

1 Introduction

It remains a great challenge in clinical oncology to detect cancer at the early stages [1–3]. There is an unmet need to develop the capability to noninvasively detect premalignant lesions so cancer preventive strategies can be successfully implemented. Hyperpolarized magnetic resonance (HP-MR) has become a major new imaging modality by providing valuable information on previously inaccessible aspects of biological processes by detecting endogenous, nontoxic 13C-labeled probes that can monitor enzymatic conversions through key biochemical pathways [4–6]. Clinical trials with this modality are ongoing at several centers all over the world [7]. HP-MR provides an exciting opportunity to identify and understand early metabolic aberrations and to enable the detection of premalignant lesions for which no methods of detection currently exist.

In conventional magnetic resonance imaging (MRI), the images of the body tissues are captured due to signal from water which is abundant in the body [8]. The other organic molecules in the body can also be captured using ^{1}H magnetic resonance spectroscopy (MRS). The physiological concentrations of other bio molecules in the body tissues is low, so it is difficult to image even with ^{1}H nuclei which is 99.98% abundant [9]. Furthermore, imaging less abundant nuclei in the molecules in the body and nuclei with smaller gyromagnetic ratio are even more difficult; however, this issue of sensitivity is addressed by HP-MR. HP-MR is a novel and developing technology that can enhance the probe signal over ~10,000-fold compared to its thermal equilibrium signal [10–13]. There are four established methods for generating hyperpolarized probes: (1) dynamic nuclear polarization (DNP) [10, 13], (2) optical pumping for hyperpolarizing noble gases [14], (3) the “brute force” approach [15], and (4) parahydrogen and synthesis allow dramatically enhanced nuclear alignment (PASADENA), which includes parahydrogen-induced polarization (PHIP) and parahydrogen-based signal amplification by reversible exchange (SABRE) [16]. The detailed description of the hyperpolarization methods can be found elsewhere [17]. DNP is the most common and widely used method for hyperpolarization. In the dynamic nuclear polarization process, magnetization is transferred from the unpaired electrons generally from added radicals to the nucleus of probe under the microwave irradiation at low temperature of 1.5 K and high magnetic field as 3 T [17]. The development of dissolution-DNP technique in 2003 [4] has opened a new avenue to perform in vivo imaging, where the fate of metabolites containing low abundant nuclei such as ^{13}C and ^{15}N can be detected and tracked [18]. The routine dissolution DNP instrument employed which carries out hyperpolarization in the preclinical setting is HyperSense (Oxford Instruments, UK) and is shown in Fig. 1a. A clinical polarizer is available for performing real-time metabolic imaging in humans (SPINLab, GE Healthcare, USA) and over 20 such polarizers have been installed around the world [19].

The most commonly used hyperpolarized probes are ^{13}C enriched, either uniformly or selectively enriched, to track the pathways of interest. ^{13}C-enriched molecules have comparatively longer relaxation time of ^{13}C nucleus compared to other nuclei. The high ^{13}C signal of the HP probes and the fact hyperpolarized signal is carried over in the products of biochemical transformation allow investigators to interrogate biochemical reactions in real time. The probes are usually part of the biochemical reactions such as energy metabolism (glucose and pyruvate) and Krebs's cycle (succinate and glutamate). So far, HP-MR experiments have been executed mostly in preclinical models and is not routinely used in the clinic. However, several clinical trials have been performed or are currently ongoing [5]. HP-MR in preclinical setting involves injecting the hyperpolarized probe—dissolved in a biocompatible solvent—into the tail vein of rodents. The probe diffuses through the blood to populate in well-perfused body tissues. After entering the extracellular fluid, the molecule is taken up into the cells with the help of endogenous transporters. All of these processes must happen before the HP signal decays, which is determined by the decay time (longitudinal relaxation time T_1) of the HP probe. For most probes, T_1 ranges from 15 to 20 s to about 2 min. Hence, it is important to dissolve the probe in the solvent immediately and inject into the animals quickly to avoid the hyperpolarization signal loss due to relaxation. The specially designed proton volume coil and ^{13}C surface coil is used to receive the signal from the enriched HP ^{13}C probe in vivo.

The utility of HP-MR is not only simply tracking the probe diffusing inside the body but also its ability to visualize downstream metabolic products of injected probes converted by endogenous enzymes [5]. We can quantify in vivo metabolic flux in real time alongside metabolic imaging. However, all process must happen within the time-frame of longitudinal relaxation time (T_1) of HP probe. Therefore, only fast biochemical reactions can be visualized.

Glycolytic breakdown of glucose is a multi-step process that eventually yields pyruvate in the cytosol. Pyruvate is the final breakdown product of glucose in glycolysis and is preferably converted to lactate in cancer cells. The high dependence of the cancer cells on glucose and glycolysis is often referred to as the Warburg effect after the initial discovery of this dependence by Dr. Otto Warburg [20]. Hence, pyruvate is a commonly used probe to interrogate abrupt energy metabolism in cancer. Another key point is pyruvate is taken up rapidly by the pyruvate transporters [21]. In the cytosol the HP [1-^{13}C] pyruvate has four important fates [22]: (1) conversion to lactate, (2) conversion to alanine, (3) transport into mitochondria and converted to carbon dioxide, and (4) conversion to Acetyl-CoA to be utilized in the Krebs/Tricarboxylic Acid (TCA) cycle (Fig. 2). When HP-pyruvate is injected into an animal, the signal is recorded from an anatomical imaging slice placed in the tissue of interest. An example of a hyperpolarized metabolic imaging spectrum is shown in Fig. 3. The flux from pyruvate to a downstream metabolite can be visualized and evaluated using either TopSpin (Bruker BioSpin GmbH, Ettingen, Germany) or MestReNova (Mestrelab Research, Santiago, Spain), in either of the two following ways:

1. Ratio of signals integrated over time (e.g. lactate/pyruvate, alanine/lactate etc.) [23].

2. *K*p (according to the Bolch equation) K_{PL} pyr → lactate, K_{PA} pyr → alanine [24].

Since pancreatic ductal adenocarcinoma (PDAC) is one of the most aggressive cancer types with no efficacious methodology for early diagnosis, it was chosen to reflect the utility of this methodology. PDAC tumors can be removed by surgery, if detected early [25]. There is unequivocal evidence that diagnosis of PDAC at earlier, resectable stages has a profoundly favorable impact on prognosis [1]. The 5-year survival of resected PDAC is as high as ~25–30% in major treatment centers, increasing to 30–60% for tumors <2 cm, and as high as 75% for minute lesions under 10 mm in size [26, 27]. Unfortunately, most patients are diagnosed at a late stage, when the tumor has advanced into local blood vessels, and other body organs, and is no longer excisable. Thus, there is an urgent call to develop non-invasive imaging modalities for early detection of PDAC, especially in high-risk patients those with familial pre-disposition, long-standing diabetes, or chronic pancreatitis [28].

PDAC is considered as a paradigm of genetically defined metabolic abnormalities. Genetic mutations trigger specific signaling pathways that are associated with metabolic transformations, which can potentially be detected by hyperpolarization methods with a high degree of sensitivity.

Recently, it has reported by Dutta et al. that aggressiveness of pancreatic cancer is directly correlated to pyruvate-to-lactate conversion using HP-MR and ex vivo ^{1}H NMR spectroscopy in a panel of well annotated patient-derived PDAC xenograft (PDX) mouse models [29]. Seminal work by Serrao et al. demonstrated a method for early detection of PanINs (pancreatic intraepithelial neoplasia) in murine models using HP-MR with [1-^{13}C] pyruvate probe. The study used genetically engineered KPC (K-Ras and p53 mutations) and KC (K-Ras mutation) mice, which develop PanIN spontaneously. In addition, wild-type mice treated with caerulein injections to induce acute pancreatitis that developed into PanINs in later stage were also employed in the HP-MR study. Animal models were imaged using HP [1-^{13}C] pyruvate at different stages of development from PanIN to PDAC precursor lesions, and the fluxes from [1-^{13}C] pyruvate to lactate and alanine were measured [23]. It is important to note that the pyruvate and lactate signals obtained here are not from the endogenous metabolites but rather from the injected pyruvate probe and the lactate derived from the probe. The information of pyruvate-to-lactate flux is valuable because it can be an indicator of the extent of glycolysis manifested in the tissue slice. The results from individual mice showed a decreasing alanine-to-lactate ratio with progression of disease from normal tissue to pancreatitis to low-grade PanIN to high-grade PanIN and finally to PDAC. Mice from all three groups follow this disease progression, although with disparate timelines. The metabolic flux pattern observed is correlated with increasing Lactate Dehydrogenase (LDH) activity and decreasing Alanine Transaminase (ALT) activity. The metabolic flux from pyruvate to lactate and alanine is minimal in normal pancreatic tissue and progressively increases with disease progression. This technique can be used to create three-dimensional metabolic maps of the pancreas to identify the extent of cancerous growth. This work was extended by Dutta et al. in our laboratories to demonstrate that real-time conversion kinetic rate constants (K_{PA} and K_{PL}) can be used as metabolic imaging biomarkers of premalignant pancreatic lesions [30]. Recently, a pilot study reported the

feasibility of HP [1-^{13}C] pyruvate MRI in PDAC patients, and no adverse effect was observed after bolus injection of pyruvate [31]. These studies reveal the potential of HP-pyruvate's conversion to lactate to be used in the early detection of PDAC.

In summary, hyperpolarization allows for high sensitivity enhancement relative to conventional magnetic resonance and is a nontoxic, nonradioactive method for assessing tissue metabolism and other physiologic properties. Here we delineate the methods and protocols used for hyperpolarized pyruvate imaging in murine models for detection of premalignant lesions. This methodology would be useful not for only for early detection but also to determine efficacy of immunopreventive strategies implemented at early stages to assess for lesions regression.

2 Materials

2.1 Genetically Engineered Mice

1. Genetically engineered mouse (GEM) models that give rise to premalignant lesions and aged-matched litter mate control animals should be employed in the study. We used the conditional P48:Cre; LSL-KRAS^{G12D} (KC) mice and as control, we used P48:Cre littermates sacrificed at the same time than experimental mice (age matched).
2. All animal experiments must be conducted in compliance with the National Institutes of Health (NIH) guidelines for animal research and protocols must be approved by the Institutional Animal Care Committee.

2.2 Hyperpolarizing [1-^{13}C] Pyruvate

1. OX063 trityl radical (GE Healthcare).
2. Neat [1-^{13}C] pyruvic acid (Isotech, Sigma-Aldrich and/or Cambridge Isotopes Laboratories).
3. Gd^{3+} (Magnevist, Bayer healthcare, Wayne, NJ).
4. DNP HyperSense polarizer (Oxford Instruments).
5. 4-(2-Hydroxyethyl)-1-piperazineethanesulfonic acid.
6. NaCl.
7. Ethylenediaminetetraacetic acid (EDTA).

2.3 Magnetic Resonance Spectroscopy

1. ^{1}H/^{13}C volume coil (OD: 75 mm, ID:40 mm, Bruker BioSpin MRI GmbH, Ettingen, Germany).
2. ^{13}C surface coil (OD: 20 mm, ID:15 mm, Doty Scientific Inc., Columbia, SC).
3. 7 T Bruker Biospec horizontal bore MR scanner (Bruker BioSpin MRI GmbH, Ettingen, Germany).
4. MATLAB (MathWorks Inc., Natick, MA).

5. TopSpin (Bruker BioSpin GmbH, Ettingen, Germany).
6. MestReNova (Mestrelab Research, Santiago, Spain).

3 Methods

3.1 Hyperpolarization Methodology

1. *Sample Preparation*: OX063 trityl radical is mixed with neat [1-^{13}C] pyruvic acid to a concentration of 15 mM. 20 μL of this solution is dissolved with 0.4 μL of 50 mM Gd^{3+} and inserted into the sample cup.
2. *Sample Insertion:* The sample cup is loaded into a DNP commercial HyperSense polarizer (Fig. 1a) and irradiated at a microwave frequency of 94.100 GHz for 40–45 min at very low temperature ~1.5 K and high magnetic field 3.35 T. The sample starts to polarize in this environment and reaches 99.9% polarization (solid-state polarization plateau) within this time range.
3. *Sample Retrieval and Dissolution for Injection*: After polarizing the pyruvate sample at solid state, the automated dissolution process brings the sample as injectable solution at 37 °C and neutral pH 7.6. In a typical experiment, 4 mL buffer solution containing 40 mM TRIS (7.6 pH preset), 80 mM NaOH, 0.1 g/L EDTA, and 50 mM NaCl is loaded into the sample recovery chamber which is heated up to 165 °C. This solution hits the super-cool solid pyruvate sample at high pressure, dissolves at 37 °C, and is ready for injection.
4. *Cleaning the dissolution stick and sample cup for the next dissolution*: 4 mL dissolution media (1% EDTA/water) is flushed out twice using the HyperSense automated sample cup cleaning module.

3.2 MRI and MRS

1. *Setting up the MRI machine for anatomic and ^{13}C MR*: All imaging and spectroscopy is performed with either a dual tuned ^{1}H/^{13}C volume coil (OD: 75 mm, ID:40 mm) or in a combination ^{1}H volume coil with a transmit/receive^{13}C surface coil (OD: 20 mm, ID:15 mm) placed directly on the region of interest of the mouse femur in a 7 T Bruker Biospec horizontal bore MR scanner (Fig. 1b).
2. *Animal Preparation*: Prior to hyperpolarization experiments, animals are anesthetized with 3% isoflurane mixed with oxygen and then maintained at 0.5–1% isoflurane and a tail vein catheter is placed to deliver the HP pyruvate solution. Animals are placed on a heated pad, and their respiration and heart rate are monitored in a computerized system during imaging procedures.
3. *Imaging Procedure*: Proton anatomic images are acquired using a multi-slice T_2-weighted RARE (Rapid Acquisition with Relaxation Enhancement) sequence. Images of different view/planes including axial, coronal, and sagittal are acquired to identify the best location of the tumors or region of interest on the mice (*see* Notes 1–3). A series of slice-selective ^{13}C spectra (field-of-view 40 × 40 mm, slice-thickness 8–10 mm) are collected right after injection of HP

[1-^{13}C] pyruvate using spFLASH sequence. A total of 90 transients are acquired with a time delay between each transient being 2 s (total time 3 min). Each transient utilized a 15–20° flip angle excitation pulse (gauss pulse) and 2048 data points (*see* Note 4).

4. *Post-acquisition Processing*: Data was processed in MATLAB (MathWorks Inc., Natick, MA), TopSpin (Bruker BioSpin GmbH, Ettingen, Germany), or MestReNova (Mestrelab Research, Santiago, Spain). The dynamic spectra are manually phased and baseline-corrected, and line-broadening is applied (10–15 Hz). The area under the spectral peaks for pyruvate and lactate are integrated over the whole array. Normalized lactate (nLac) ratio is calculated as lactate over the sum of pyruvate and lactate signals [25] as by this equation.

$$\mathrm{nLac} = \frac{\int([\mathrm{Lactate}])dt}{\int([\mathrm{Lactate}] + [\mathrm{Pyruvate}])dt}$$

The metabolic flux ratios of pyruvate to lactate can also be determined using a unidirectional model where the apparent rate constant $K_{\mathrm{Pyr}\rightarrow\mathrm{Lact}}$ can be determined.

4 Notes

1. The imaging parameters of the T_2-weighted scans are: echo time T_E = 17 ms, repetition time T_R = 2.5 s, 4 cm field of view, 256 μm × 256 μm in-plane resolution, ten to fifteen 1–1.5 mm slices, and 4 averages.

2. For orthotopic pancreatic cancer models, we place the spectroscopic slice cutting through the pancreas, and covering the entire abdominal section. This means that the pyruvate and lactate signals acquired are derived from both the pancreas and the surrounding tissue. However, the surrounding tissue and the normal pancreatic tissue do not produce significant lactate signal, and hence, the lactate signal acquired is assumed to be primarily from the cancerous tissue only. This choice of whole-abdomen imaging is due to lack of a sequence that could focus the image on the pancreas.

   With the heterotopic (flank tumors) of pancreatic cancer, a challenge to imaging is posed by necrotic cores of large tumors (>15 mm diameter). Hence, we usually run our protocols on small (size ~7.5 mm diameter), non-necrotic tumors and by placing the slice through the non-necrotic periphery (Fig. 2).

3. While taking proton images (T_2-weighted Rapid Acquisition with Relaxation Enhancement (RARE) sequence) to locate pancreas of animal, keep trigger on and adjust animal breathing such that breaths/minute should be less than repetition time (TR) to avoid motion artifacts in the image.

4. A small 8 M ^{13}C-urea phantom doped with gadolinium-DPTA is placed in each mouse experiment for chemical shift referencing.

Acknowledgments

This work was supported by grants from the National Institutes of Health (P50CA094056, U01CA214263, R01CA218004, U54CA151668, and R21CA185536 to P.B.), an Institutional Research Grant (to P.B.), Pancreatic Cancer Action Network (PANCAN) (16-65-BHAT to P.B., F.M.), Duncan Family Institute (to P.B.), NCI DCP PREVENT Preclinical Drug Development Program: Preclinical Efficacy and Intermediate Biomarkers; Contract 75N91019D00021 (to P.B., F.M.),startup grants from the University of Texas MD Anderson Cancer Center (to P.B., F. M.), Cancer Prevention & Research Institute of Texas (CPRIT) Award (RP180164 to P.B. and RR180012 and RP200526 to S.S.) and generous philanthropic contributions to Koch Foundation Genitourinary Medical Oncology Funds (to P.B.). This work was also supported by a CPRIT Research Training Grant Award (RP170067 to T.C.S.), National Institutes of Health National Cancer Institute Training Grant Award (2T32CA096520 to D. B.), and a Gulf Coast Consortia/Keck Center CCBTP postdoctoral fellowship (CPRIT RP170593 to S.P.). M.T. acknowledges support from the Neubauer Family Foundation. We also thank Drs. Richard Behringer and Rachel Miller, Instructors of G&E Scientific Writing Course at MD Anderson Cancer Center. This work also was supported by the National Institutes of Health/NCI Cancer Center Support Grant under award number P30 CA016672 to MD Anderson Cancer Center.

References

1. Blackford AL, Canto MI, Klein AP, Hruban RH, Goggins M (2020) Recent trends in the incidence and survival of stage 1A pancreatic cancer: a surveillance, epidemiology, and end results analysis. J Natl Cancer Inst 112 (11):1162–1169. 10.1093/jnci/djaa004 [PubMed: 31958122]
2. Rahib L, Smith BD, Aizenberg R, Rosenzweig AB, Fleshman JM, Matrisian LM (2014) Projecting cancer incidence and deaths to 2030: the unexpected burden of thyroid, liver, and pancreas cancers in the United States. Cancer Res 74(11):2913–2921 [PubMed: 24840647]
3. Siegel RL, Miller KD, Jemal A (2020) Cancer statistics, 2020. CA Cancer J Clin 70(1):7–30 [PubMed: 31912902]
4. Ardenkjær-Larsen JH, Fridlund B, Gram A, Hansson G, Hansson L, Lerche MH et al. (2003) Increase in signal-to-noise ratio of> 10,000 times in liquid-state NMR. Proc Natl Acad Sci U S A 100(18):10158–10163 [PubMed: 12930897]
5. Dutta P, Salzillo TC, Pudakalakatti S, Gammon ST, Kaipparettu BA, McAllister F et al. (2019) Assessing therapeutic efficacy in real-time by hyperpolarized magnetic resonance metabolic imaging. Cell 8(4):340
6. Dutta P, Martinez GV, Robert J, Gillies RJ (2013) A new horizon of DNP technology: application to in-vivo ^{13}C magnetic resonance spectroscopy and imaging. Biophys Rev 5 (3):271–281 [PubMed: 26491489]
7. Kurhanewicz J, Vigneron DB, Ardenkjaer-Larsen JH, Bankson JA, Brindle K, Cunningham CH et al. (2019) Hyperpolarized ^{13}C MRI: path to clinical translation in oncology. Neoplasia 21(1):1–16 [PubMed: 30472500]
8. McRobbie DW, Moore EA, Graves MJ, Prince MR (2017) MRI from picture to proton, 3rd edn. Cambridge University Press, Cambridge
9. Barker PB, Bizzi A, De Stefano N, Gullapalli R, Lin DDM (2009) Clinical MR spectroscopy: techniques and applications. Cambridge University Press, Cambridge
10. Overhauser AW (1953) Polarization of nuclei in metals. Phys Rev 92(2):411–415. 10.1103/PhysRev.92.411
11. Carver TR, Slichter CP (1953) Polarization of nuclear spins in metals. Phys Rev 92 (1):212–213. 10.1103/PhysRev.92.212.2
12. Abragam A, Goldman M (1978) Principles of dynamic nuclear polarisation. Rep Prog Phys 41(3):395–467
13. Nikolaou P, Goodson BM, Chekmenev EY (2015) NMR hyperpolarization techniques for biomedicine. Chem Eur J 21 (8):3156–3166. 10.1002/chem.201405253 [PubMed: 25470566]
14. Walker TG, Happer W (1997) Spin-exchange optical pumping of noble-gas nuclei. Rev Mod Phys 69(2):629–642. 10.1103/RevModPhys.69.629
15. Hirsch ML, Kalechofsky N, Belzer A, Rosay M, Kempf JG (2015) Brute-force hyperpolarization for NMR and MRI. J Am Chem Soc 137 (26):8428–8434. 10.1021/jacs.5b01252 [PubMed: 26098752]

16. Hövener JB, Pravdivtsev AN, Kidd B, Bowers CR, Glöggler S, Kovtunov KV et al. (2018) Parahydrogen-based hyperpolarization for biomedicine. Angew Chem Int Ed 57 (35):11140–11162
17. Viale A, Reineri F, Santelia D, Cerutti E, Ellena S, Gobetto R et al. (2009) Hyperpolarized agents for advanced MRI investigations. Q J Nucl Med Mol Imaging 53(6):604 [PubMed: 20016452]
18. Golman K, Lerche M, Pehrson R, Ardenkjaer-Larsen JH (2006) Metabolic imaging by hyperpolarized 13C magnetic resonance imaging for in vivo tumor diagnosis. Cancer Res 66 (22):10855–10860 [PubMed: 17108122]
19. Lin C, Salzillo TC, Bader DA, Wilkenfeld SR, Awad D, Pulliam TL et al. (2019) Prostate cancer energetics and biosynthesis. Adv Exp Med Biol 1210:185–237 [PubMed: 31900911]
20. Warburg O (1956) On the origin of cancer cells. Science 123(3191):309–314 [PubMed: 13298683]
21. Rao Y, Gammon S, Zacharias NM, Liu T, Salzillo T, Xi Y et al. (2020) Hyperpolarized [1-^{13}C]pyruvate-to-[1-^{13}C]lactate conversion is rate-limited by monocarboxylate transporter-1 in the plasma membrane. Proc Natl Acad Sci U S A 117(36):22378 [PubMed: 32839325]
22. Düwel S, Hundshammer C, Gersch M, Feuerecker B, Steiger K, Buck A et al. (2017) Imaging of pH in vivo using hyperpolarized ^{13}C-labelled zymonic acid. Nat Commun 8 (1):15126 [PubMed: 28492229]
23. Serrao EM, Kettunen MI, Rodrigues TB, Dzien P, Wright AJ, Gopinathan A et al. (2016) MRI with hyperpolarised [1–13C] pyruvate detects advanced pancreatic preneoplasia prior to invasive disease in a mouse model. Gut 65(3):465–475 [PubMed: 26347531]
24. Zierhut ML, Yen Y-F, Chen AP, Bok R, Albers MJ, Zhang V et al. (2010) Kinetic modeling of hyperpolarized [1-^{13}C]pyruvate metabolism in normal rats and TRAMP mice. J Magn Reson 202(1):85–92 [PubMed: 19884027]
25. Chari ST, Kelly K, Hollingsworth MA, Thayer SP, Ahlquist DA, Andersen DK et al. (2015) Early detection of sporadic pancreatic cancer: summative review. Pancreas 44(5):693 [PubMed: 25931254]
26. Lennon AM, Wolfgang CL, Canto MI, Klein AP, Herman JM, Goggins M et al. (2014) The early detection of pancreatic cancer: what will it take to diagnose and treat curable pancreatic neoplasia? Cancer Res 74(13):3381–3389 [PubMed: 24924775]
27. Ryan DP, Hong TS, Bardeesy N (2014) Pancreatic adenocarcinoma. New Engl J Med 371 (11):1039–1049 [PubMed: 25207767]
28. Cancer SW (2019) Facts & Figures 2019. American Cancer Society, Atlanta, GA, USA
29. Dutta P, Perez MR, Lee J, Kang Y, Pratt M, Salzillo TC et al. (2019) Combining hyperpolarized real-time metabolic imaging and NMR spectroscopy to identify metabolic biomarkers in pancreatic Cancer. J Proteome Res 18 (7):2826–2834. 10.1021/acs.jproteome.9b00132 [PubMed: 31120258]
30. Dutta P, Pando SC, Mascaro M, Riquelme E, Zoltan M, Zacharias NM et al. (2020) Early detection of pancreatic intraepithelial Neoplasias (PanINs) in transgenic mouse model by hyperpolarized (13)C metabolic magnetic resonance spectroscopy. Int J Mol Sci 21(10):3722
31. Stødkilde-Jørgensen H, Laustsen C, Hansen ESS, Schulte R, Ardenkjaer-Larsen JH, Comment A et al. (2020) Pilot study experiences with hyperpolarized [1–13C]pyruvate MRI in pancreatic Cancer patients. J Magn Reson Imaging 51(3):961–963 [PubMed: 31368215]

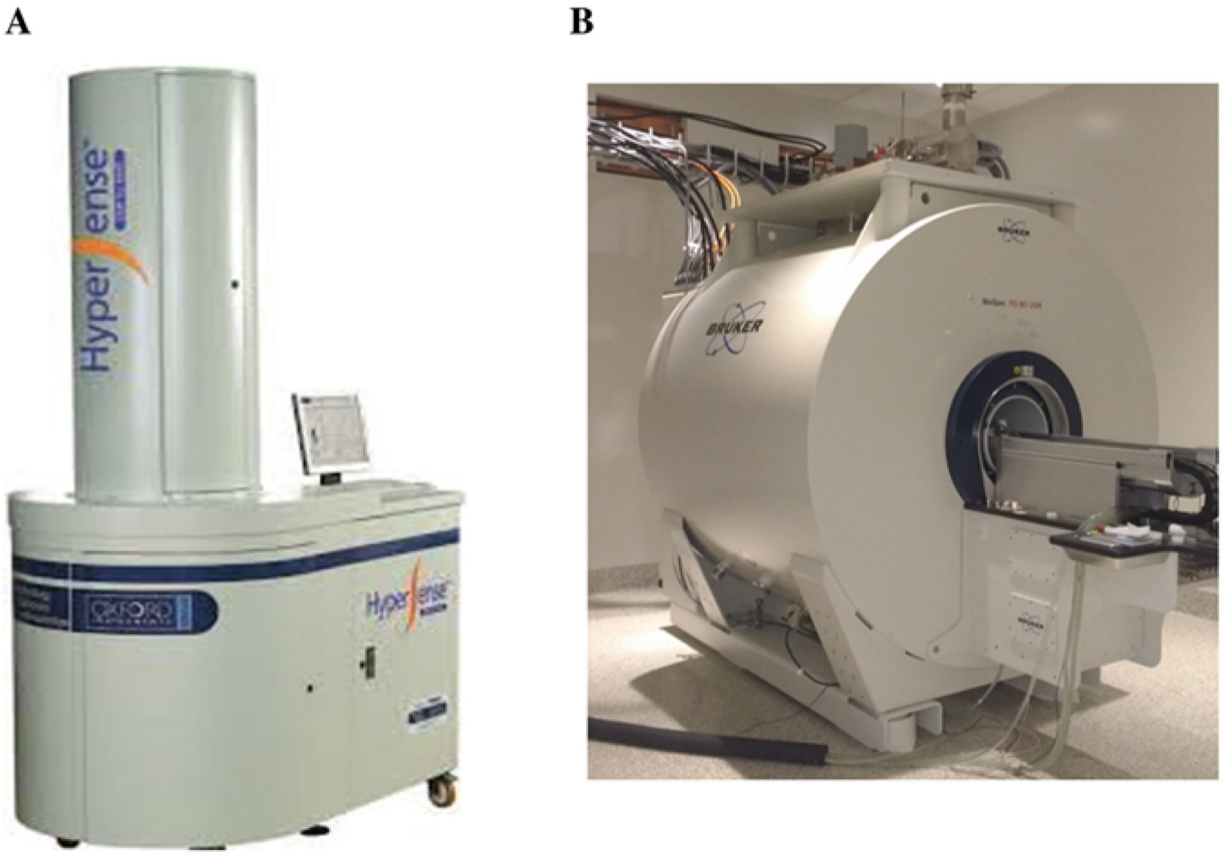

Fig. 1.

(**a**) Photo of a HyperSense DNP system. The cabinet at the bottom is engineered to achieve temperatures near 1 K, where ^{13}C sample doped with free radical is irradiated with microwaves to achieve solid-state hyperpolarization. The upper cabinet is used for sample insertion and retrieval, with the help of a long tube that is fitted with sample cup. (**b**) A preclinical Bruker 7 T MRI scanner. Due to the short decay time of HP pyruvate probe (less than 120 s), the HyperSense and MRI scanner must be in proximity, to allow instant injection of probe following hyperpolarization. In the setup at our laboratory, the two pieces of equipment are separated by a wall, which contains a small aperture for delivering the HP probe through a plastic hose

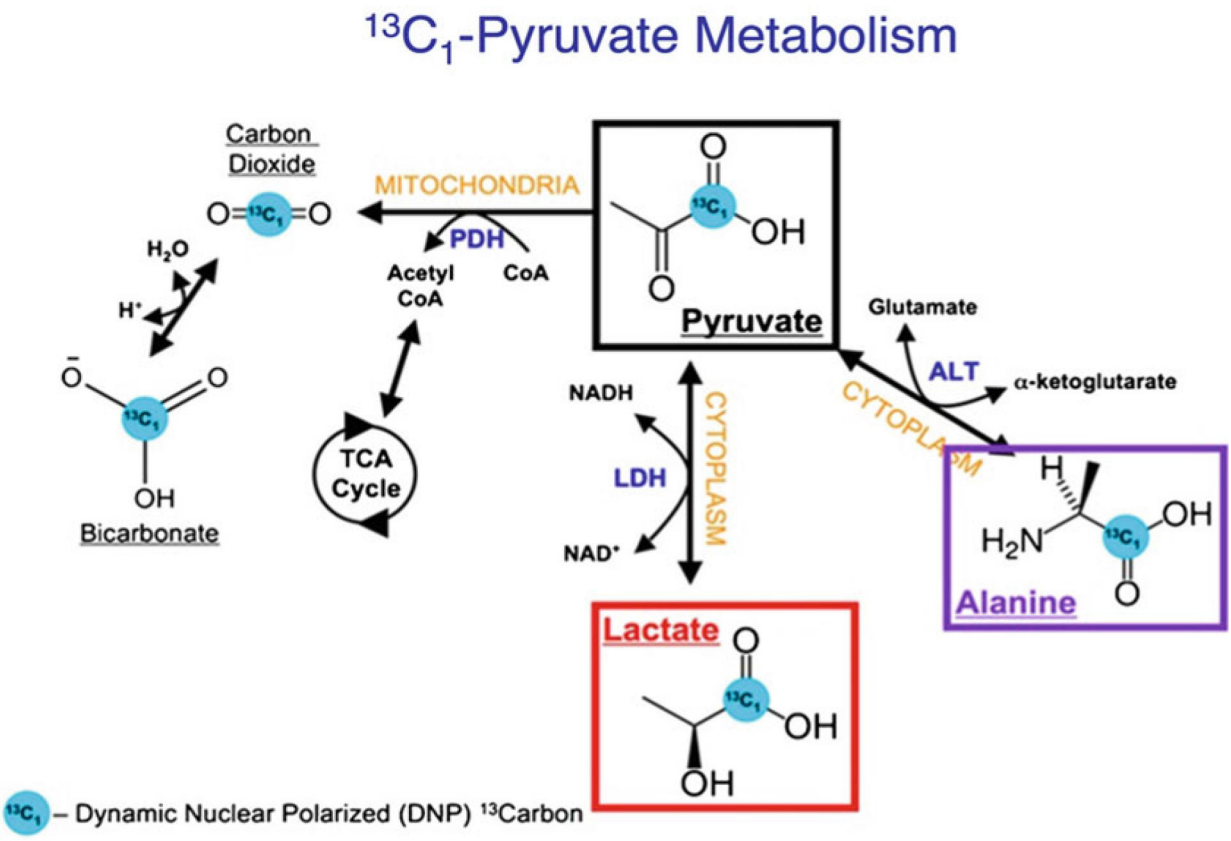

Fig. 2.

Schematic showing pyruvate metabolism inside a cell. The [1-^{13}C] pyruvate can be converted to ^{13}C-lactate, ^{13}C-alanine, and ^{13}C-bicarbonate in the presence of enzymes lactate dehydrogenase-A (LDHA), alanine transferase (ALT), and pyruvate decarboxylase respectively. (Figure adapted with permission from [6])

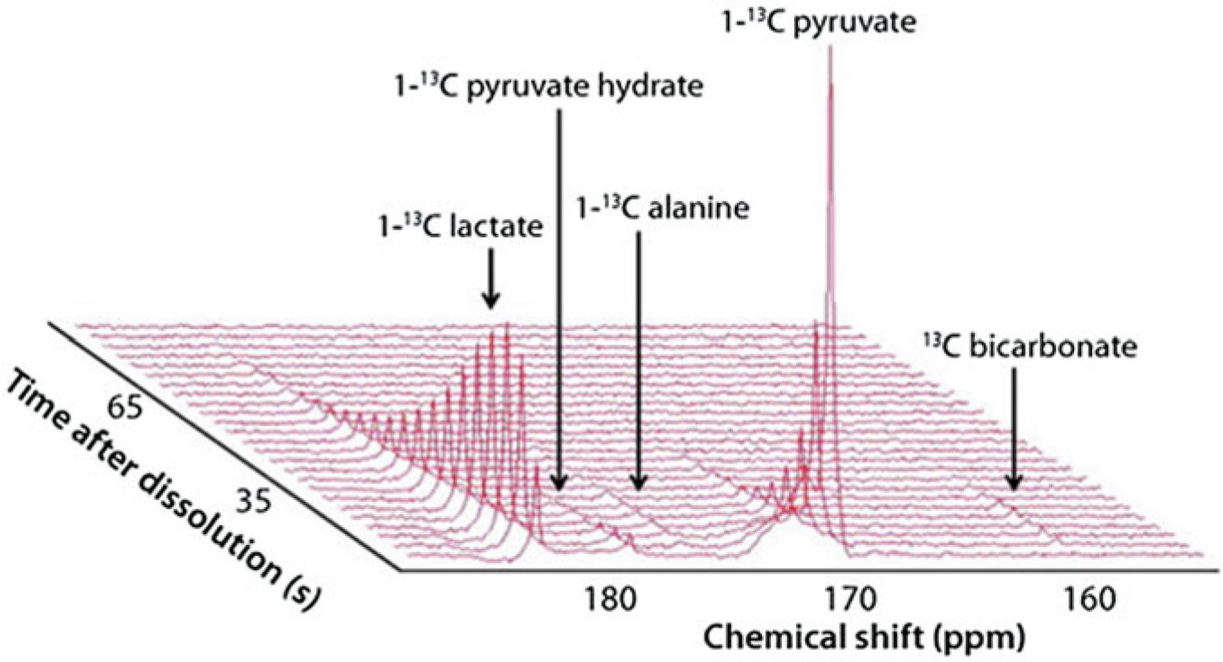

Fig. 3.

Downstream products of pyruvate metabolism such as lactate and alanine can be imaged using HP-MR. A three-dimensional, real-time readout of the signals, such as this one shown below, can be created using standard software such as MestReNova. http://www.sigmaaldrich.com/technical-documents/articles/stable-isotopes/probing-brain-metabolism-in-vivo.html. (Figure adapted with permission from Millipore Sigma-Aldrich)